Society for Endocrinology
European Society of Endocrinology

Endocrine Connections (2024) **13** e240292
https://doi.org/10.1530/EC-24-0292

Received 18 June 2024
Accepted 20 September 2024
Available online 20 September 2024
Version of Record published 29 October 2024

RESEARCH

Longitudinal changes of serum metabolomic profile after laparoscopic sleeve gastrectomy in obesity

Shuqi Li[1,*], Chenye Shi[2,*], Haifu Wu[2,*], Hongmei Yan[1], Mingfeng Xia[1], Heng Jiao[2], Yang He[1], Ming Zhong[3], Wenhui Lou[2], Xin Gao[1], Hua Bian[1] and Xinxia Chang[1]

[1]Department of Endocrinology, Zhongshan Hospital, Fudan University, Shanghai, China
[2]Department of General Surgery, Zhongshan Hospital, Fudan University, Shanghai, China
[3]Department of Critical Care Medicine, Zhongshan Hospital, Fudan University, Shanghai, China

Correspondence should be addressed to X Gao or H Bian or X Chang: gao.xin@zs-hospital.sh.cn or bian.hua@zs-hospital.sh.cn or chang.xinxia@zs-hospital.sh.cn

*(S Li, C Shi, and H Wu contributed equally to this work)

Abstract

Background: Bariatric surgery induces significant weight loss, increases insulin sensitivity, and improves dyslipidemia. As one of the most widely performed bariatric surgeries, laparoscopic sleeve gastrectomy (LSG) is thought to improve the metabolic profile along with weight loss. The objective of this study was to evaluate longitudinal changes in the serum metabolite levels after LSG and elucidate the underlying mechanisms of metabolic improvement.

Methods: Clinical metabolic parameters and serum samples were collected preoperatively and at 1, 3, and 6 months postoperatively from nine patients with obesity undergoing LSG. Serum metabolites were measured using a non-targeted metabolic liquid chromatography–mass spectrometry method.

Results: During the 1, 3, and 6 months postoperative follow-up, the body mass index, HOMA-IR, and liver fat content showed a gradual descending trend. A total of 328 serum metabolites were detected, and 38 were differentially expressed. The up-regulated metabolites were mainly enriched in ketone body metabolism, alpha-linolenic acid and linoleic acid metabolism, pantothenate and CoA biosynthesis, glycerolipid metabolism, and fructose and mannose degradation, while the down-regulated metabolites were closely related to caffeine metabolism, oxidation of branched-chain fatty acids, glutamate metabolism, and homocysteine degradation. Notably, nine metabolites (oxoglutarate, 2-ketobutyric acid, succinic acid semialdehyde, phthalic acid, pantetheine, eicosapentaenoate, 3-hydroxybutanoate, oxamic acid, and dihydroxyfumarate) showed persistent differential expression at 1, 3, and 6 months follow-up. Some were found to be significantly associated with weight loss, insulin resistance improvement, and liver fat content reduction.

Conclusions: This finding may provide a new perspective for revealing novel biomarkers and mechanisms of metabolic improvement in obesity and related comorbidities.

Keywords: bariatric surgery; metabolomics; obesity; metabolic improvement

Published by Bioscientifica Ltd.
https://ec.bioscientifica.com

Endocrine Connections (2024) **13** e240292
https://doi.org/10.1530/EC-24-0292

Introduction

The obesity epidemic is a major global health challenge in modern societies, with a global prevalence of 14% by 2020, and it is even expected to reach 24% by 2035 (https://data.worldobesity.org/publications/?cat=19). Compared to behavioral therapy and pharmacotherapy, bariatric surgery is currently the most effective and durable treatment for morbid obesity (1, 2). Laparoscopic sleeve gastrectomy (LSG) is one of the most widely performed bariatric surgeries at present (3). In addition to the primary objective of weight loss, LSG has also been shown to provide long-term solutions to related health problems, such as relief from type 2 diabetes mellitus (T2DM) (4), dyslipidemia (5), cardiovascular disease (6), and non-alcoholic fatty liver disease (NAFLD) (7), as well as a reduction in overall mortality (8). However, the exact mechanisms underlying these effects remain unclear.

Morbidly obese patients undergoing bariatric surgery often share a common metabolic background and similar environmental factors (9). Several attempts have been made to describe the mechanisms of metabolic improvement in obesity after bariatric surgery, while the effect is far from being mechanistic and includes modulation of neural circuits, alterations in the intestinal microbiome, variations in bile acid excretion, restoration of the intestinal and adipose tissue hormonal milieu, and recruitment of intestinal glucose transport molecules (10, 11, 12). Previous studies on these mechanisms mainly focused on the exploration of upstream genomics, transcriptomics, and proteomics. The recent application of metabolomics in medical research has enabled the development of metabolic biomarkers and the elucidation of physiological mechanisms underlying various diseases (13). Elucidation of systemic metabolic changes after bariatric surgery is important to gain insights into new management strategies for obesity and related comorbidities (14, 15).

Because a short-term single comparison is underrepresented, longitudinal follow-up may be a more effective way to elucidate the underlying mechanisms of metabolic improvement after bariatric surgery. Therefore, this study set up a cohort that focused on longitudinal changes in the serum metabolomic profile after LSG.

Materials and methods

Subjects

The inclusion criteria were in accordance with the guidelines of the Chinese Society for Metabolic and Bariatric Surgery. Patients aged 18–65 years with body mass index (BMI) ≥ 32.5 kg/m^2 or 27.5 ≤ BMI < 32.5 kg/m^2 plus one or more comorbidities (T2DM, dyslipidemia, hypertension, and obstructive sleep apnea) and non-surgical treatments that failed to achieve the desired weight loss or manage complications were invited to participate in this study. Finally, nine individuals (four males and five females) who underwent LSG at Zhongshan Hospital, Fudan University, between December 2014 and December 2016, were recruited into our cohort and completed the entire follow-up. Initially, all patients were obese, and all surgeries were performed by the same surgeon. Follow-up assessments were conducted at baseline (pre-surgery) and 1-, 3-, and 6-month post surgery. Anthropometric measurements, clinical biochemical parameters, and blood serum metabolome data were collected during each follow-up period.

This study was approved by the Ethical Review Committees of Zhongshan Hospital, Fudan University (No.: B2021-157R), and the study protocol adhered to the Declaration of Helsinki. Oral and written informed consent was obtained from all patients.

Clinical indicators and biochemical measurements

Body height and weight were measured using a height-weight scale, with participants removing their shoes and outer clothing. Blood pressure was measured in the right arm three times using the standard brachial cuff technique after at least 5 min of rest in a seated position, with an interval of 1 min between each measurement. The three readings were averaged for analysis.

Venous blood samples for biochemical measurements were obtained after a fasting period of at least 12 h. Serum samples were centrifuged and stored at −80°C until analysis. The serum total cholesterol (TC), high-density lipoprotein cholesterol (HDL-C), and triglyceride (TG) levels were measured using the oxidase method on a 7600 automated bioanalyzer (Hitachi). Low-density lipoprotein cholesterol (LDL-C) was calculated using the Friedewald equation. Glycosylated hemoglobin (HbA1c) levels were determined using high-pressure liquid chromatography on the Variant™ II machine (Bio-Rad). Plasma glucose levels were measured using the glucose oxidase method. Serum insulin concentration was determined by Auto DELFIA fluoroimmunoassay. The homeostatic model assessment of insulin resistance (HOMA-IR) was calculated as fasting glucose (mmol/L) × fasting insulin (mU/mL)/22.5. Liver fat content was defined as the ratio of area lipid (AL) to AL plus area water (AW) and was measured using hydrogen proton magnetic resonance spectroscopy (^{1}H-MRS) (16).

Metabolomics profiling of serum samples

Sample preparation

The serum (100 µL) was mixed with 400 µL methanol/acetonitrile (1/1, v/v) by vortexing for 30 s.

The mixture was then sonicated for 10 min at 4°C. After 1 h of incubation at −20°C, the samples were centrifuged at 18,832 ***g*** for 15 min at 4 °C. The supernatant was transferred to a new tube and evaporated to dryness at 4°C using a vacuum concentrator. The samples were reconstituted in 100 µL of acetonitrile/H_2O solution (1/1, v/v) for injection analysis. The injection volume used was 3 µL.

Chromatographic and mass spectrometry conditions

Serum metabolites were analyzed using a Shimadzu Prominence UPLC system (Nexera UHPLC LC-30A, Kyoto, Japan) interfaced with an AB SCIEX Triple TOF 5600+ system (AB Sciex, Singapore) equipped with an ESI source. Metabolites were separated using a HILIC column (ZIC-pHILIC, 5 µm, 2.1 × 100 mm, PN: 1.50462.0001, Millipore) with the column temperature maintained at 40°C. The mobile phase consisted of 25 mM ammonium acetate in 25 mM ammonia water (mobile phase A) and acetonitrile (90/10, v/v) (mobile phase B) and was run at a flow rate of 0.3 mL/min. The gradient was as follows: 95% B for 1 min, 65% B for 14 min, 40% B for 16 min, held for 18 min, then increased to 95% B for 18.1 min, then back to 9% B, and held for another 23 min. The flow rate for mobile phases was set at 0.3 mL/min. The mass spectrometer was run in positive information-dependent acquisition (IDA) mode, with the source temperature at 550°C, ion source gases 1 and 2 at 55 psi, curtain gas at 35 psi, collision energy at +30 eV or −30 eV, ion spray voltage floating at 5.5 kV or −4.5 kV, and a mass range at 60–1250 *m*/*z*. The accumulation time for the full scan was set at 150 ms, for each IDA scan, it was 45 ms. Peaks of metabolites with intensities greater than 100 c.p.s., after adding up the signal from ten rounds of IDA scans, were chosen for further analysis.

Data processing and metabolite identification

After the data were acquired, the SCIEX OS software was used to perform peak quantification and identification, integration, and retention time correction. MetaboAnalyst 5.0 (https://www.metaboanalyst.ca/) was used to process the data, including alignment, deconvolution, normalization, and data scaling. Internal standard peaks and known false-positive peaks were removed from the data matrix to reduce redundancy and pool similar peaks. In the data matrix, a minimum of 80% of the metabolic features detected across any set of samples were preserved. Following the exclusion of samples with metabolite levels falling below the quantification threshold, the lowest metabolite value was approximated. Each metabolic signature was then normalized based on its total sum. To mitigate errors arising from sample preparation and instrument fluctuations, the intensity of mass spectrometry peaks was standardized using the sum-normalization approach. Z-score normalization was applied for data scaling. The metabolite identification process commenced by matching the retention times (RTs) of detected peaks against the RTs of known metabolites. Concurrently, a comparison was made between the mass-to-charge ratios (*m*/*z*) of the detected peaks and those of the known metabolites. Peaks that met the initial RT and *m*/*z* matching criteria underwent further analysis through secondary mass spectrometry. Peaks exhibiting high similarity scores in this analysis were regarded as providing robust evidence for the identity of the corresponding metabolites. For this process, we used the AB SCIEX commercial library and the local library to confirm the identity of the metabolites.

Statistical analysis

SPSS software (version 25.0) was used for statistical analysis of anthropometric and biochemical measurements. Normality tests were first performed for quantitative variables. Normally distributed variables are expressed as mean ± S.D., and paired *t*-tests were used to compare continuous variables between groups. Multiple groups of quantitative data were compared using analysis of variance. Next, partial least squares discriminant analysis (PLS-DA) was used for differential analysis of metabolomics, and a five-fold cross-validation method was performed to evaluate model stability. Metabolites with a variable importance (VIP) score >1 in the PLS-DA model, $P < 0.05$, and fold change (FC) values ≥2 or ≤0.5 were defined as differentially expressed metabolites (DEMs). The *P*-value was generated using paired *t*-test in the R language, and the post-hoc tests were corrected using the Benjamini–Hochberg false discovery rate test. Time-series cluster analysis and heat maps were generated using the bioinformatics website (https://www.bioinformatics.com.cn/). Pathway enrichment analysis was performed using MetaboAnalyst 5.0, and the Small Molecule Pathway Database (SMPDB) was used for metabolic pathway annotation. Line charts depicting the variation trends of the continuously changing DEMs were generated using GraphPad Prism 8. $P < 0.05$ was considered statistically significant.

Results

Demographic and clinical characteristics

The demographic, clinical characteristics, and metabolic parameters of the patients pre-surgery and 1-, 3-, 6-month post-surgery are shown in Table 1. Compared with baseline, the BMI, HOMA-IR, and liver fat content of the patients decreased significantly at the three

Endocrine Connections (2024) **13** e240292
https://doi.org/10.1530/EC-24-0292

Table 1 Clinical characteristics and metabolic parameters for the patients pre- and post-surgery.

	Pre-surgery	Post-surgery		
	Baseline	1 month later	3 months later	6 months later
Sample size	9	9	9	9
Sex (male/female)	4/5	–	–	–
Age (years)	40.33 ± 4.55	–	–	–
BMI (kg/m^2)	43.60 ± 2.41	37.75 ± 2.15	34.09 ± 2.21[b]	30.75 ± 2.04[b,c]
SBP (mm Hg)	131.11 ± 6.38	137.33 ± 5.41	122.44 ± 5.19	129.33 ± 6.22
DBP (mm Hg)	84.78 ± 4.61	81.22 ± 4.26	76.22 ± 3.90	80.44 ± 2.86
FBG (mmol/L)	6.74 ± 1.39	5.04 ± 0.83	4.53 ± 0.23	4.58 ± 0.32
HbA1c (%)	6.13 ± 0.45	5.70 ± 0.37	5.24 ± 0.20	5.37 ± 0.21
HOMA-IR	6.25 ± 1.22	1.86 ± 0.46[b]	1.73 ± 0.29[b]	1.25 ± 0.25[b]
TC (mmol/L)	3.82 ± 0.34	3.71 ± 0.27	3.88 ± 0.19	4.21 ± 0.19
TG (mmol/L)	1.67 ± 0.35	0.97 ± 0.07	1.06 ± 0.12	0.91 ± 0.10
LDL-C (mmol/L)	2.24 ± 0.19	2.29 ± 0.26	2.28 ± 0.13	2.46 ± 0.17
HDL-C (mmol/L)	1.15 ± 0.05	0.97 ± 0.05	1.11 ± 0.08	1.33 ± 0.08[d,e]
Liver fat content (%)	35.9% ± 7.7%	18.7% ± 3.5%[a]	14.6% ± 2.1%[b]	8.3% ± 1.9%[b]

[a]P < 0.05 compared with baseline; [b]P < 0.01 compared with baseline; [c]P < 0.05 compared with 1 month; [d]P < 0.01 compared with 1 month; [e]P < 0.05 compared with 3 months.
BMI, body mass index; DBP, diastolic blood pressure; FBG, fasting blood glucose; HDL-C, high-density lipoprotein cholesterol; HOMA-IR, homeostasis model assessment-insulin Resistance; LDL-C, low-density lipoprotein cholesterol; SBP, systolic blood pressure; TC, total cholesterol; TG, triglyceride.

postoperative follow-up points (P < 0.05). Compared to 1 and 3 months after surgery, the HDL-C level of the patients increased significantly at 6 months after surgery (P < 0.05).

Characteristics of metabolome profile pre- and post-LSG

Liquid chromatography–mass spectrometry (LC–MS) metabolomics was conducted on 36 serum samples from nine patients at four time points: pre-surgery, 1-, 3-, and 6-month post surgery. In total, 328 metabolites were identified in serum metabolomes. After normalization by the baseline group and data scaling (mean-centered and divided by the S.D. of each variable), the PLS-DA plot showed that these four groups (pre-surgery, 1-, 3-, and 6-month post surgery) clustered in different directions, indicating that there were significant differences in metabolite profiles among the four groups (Fig. 1).

Identification of differentially expressed metabolites

Through differential expression analysis, metabolites with P-values <0.05, VIP values >1, and FC values ≥2 or ≤0.5 were defined as DEMs. Finally, 38 metabolites were found to have significantly changed compared with baseline throughout the entire postoperative follow-up, mainly including amino acids, lipids, energy-related metabolites, and gut microbiota-related metabolites. Among them, 19 metabolites exhibited statistically significant changes at 1-month post surgery (ten up-regulated and nine down-regulated), 21 metabolites exhibited statistically significant changes at 3 months post surgery (15 up-regulated and six down-regulated), and 11 metabolites exhibited statistically significant changes at 6 months post surgery (eight up-regulated and three down-regulated) (Fig. 2).

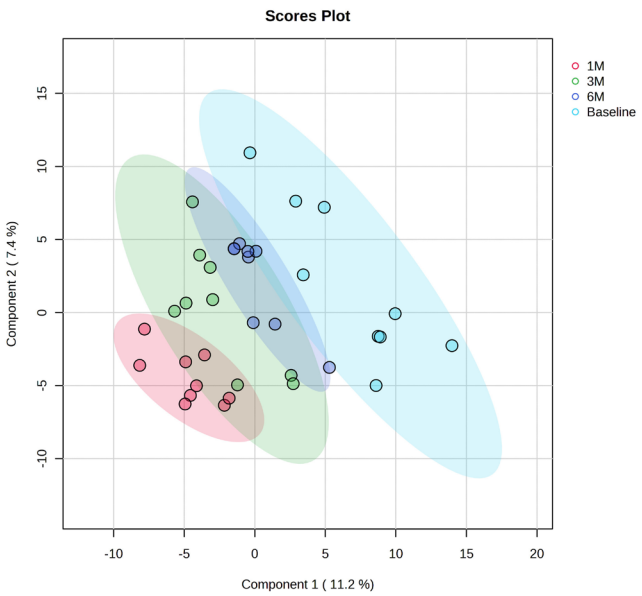

Figure 1

PLS-DA plot of baseline (pre-surgery), 1-month post surgery, 3-month post surgery, and 6-month post surgery. The *X*-axis and *Y*-axis are labeled with PC1 (the first principal component) and PC2 (the second principal component).

Endocrine Connections (2024) **13** e240292
https://doi.org/10.1530/EC-24-0292

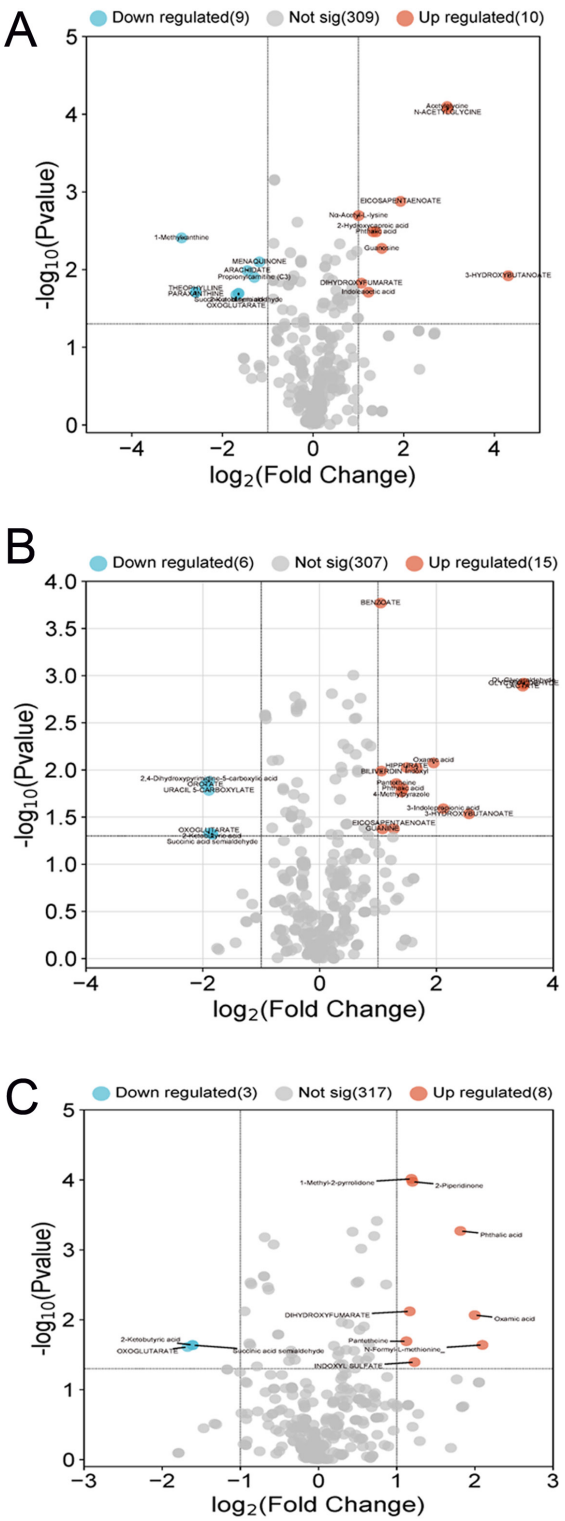

Figure 2

Volcano plot of metabolite abundance changes at 1-month post surgery (A), 3-month post surgery (B), and 6-month post surgery (C). Red points mean $P < 0.05$ and fold change (FC) ≥2 compared with baseline (up-regulated metabolites), blue points mean $P < 0.05$ and FC ≤ 0.5 compared with baseline (down-regulated metabolites), gray points mean not significant.

Time-series cluster and pathway enrichment analysis of DEMs

According to the time-series cluster analysis, all 38 DEMs were classified into four main clusters based on their response after surgery. Cluster 1, consisting of 12 metabolites, showed a gradual decline throughout the follow-up period, whereas cluster 4, containing eight metabolites, exhibited a consistent increasing trend. Cluster 2, containing eight metabolites, initially increased in the first month before returning to near-baseline levels over the entire 6-month period. Cluster 3, containing ten metabolites, gradually increased from baseline to 3 months after surgery and then returned to near-baseline levels at 6 months (Fig. 3A). The heat maps of the four clusters visually showed different variation trends during follow-up (Fig. 3B). To explore the metabolic pathways, enrichment analysis was conducted on the four clusters, and the metabolic pathways were presented according to the enrichment degrees from high to low (Fig. 3C). The most significantly enriched metabolic pathways in cluster 1 were caffeine metabolism, oxidation of branched-chain fatty acids, glutamate metabolism, and homocysteine degradation. Then, ketone body metabolism, alpha-linolenic acid, and linoleic acid metabolism were the main pathways enriched in cluster 2. Glycerolipid metabolism, fructose and mannose degradation, and gluconeogenesis were the main pathways enriched in cluster 3. Cluster 4 was mainly enriched in pantothenate and CoA biosynthesis, and propanoate metabolism. The specific metabolites in each cluster are shown in Fig. 3D.

The characteristics of continuously changing DEMs and the correlation with metabolic improvement

In all DEMs, compared with baseline, two metabolites (3-hydroxybutanoate and eicosapentaenoate) showed significant alterations at both 1- and 3-month post surgery points, one metabolite (dihydroxyfumarate) changed at both the 1- and 6-month points, two metabolites (pantetheine and oxamic acid) changed at both 3- and 6-month points, and four metabolites (phthalic acid, oxoglutarate, 2-ketobutyric acid, and succinic acid semialdehyde) changed at all three postoperative time points. These metabolites were called continuously changing DEMs (Fig. 4). The variation trends of the nine continuously changing DEMs are shown in Fig. 5. To explore the potential link between these nine DEMs and metabolic improvement, a correlation analysis was performed between the nine DEMs and clinical parameters. The results showed that phthalic acid levels were significantly negatively correlated with BMI. Oxoglutarate, 2-ketobutyric acid, and succinic acid semialdehyde levels were significantly positively correlated with HOMA-IR and liver fat content. Additionally, 3-hydroxybutanoate

Endocrine Connections (2024) **13** e240292
https://doi.org/10.1530/EC-24-0292

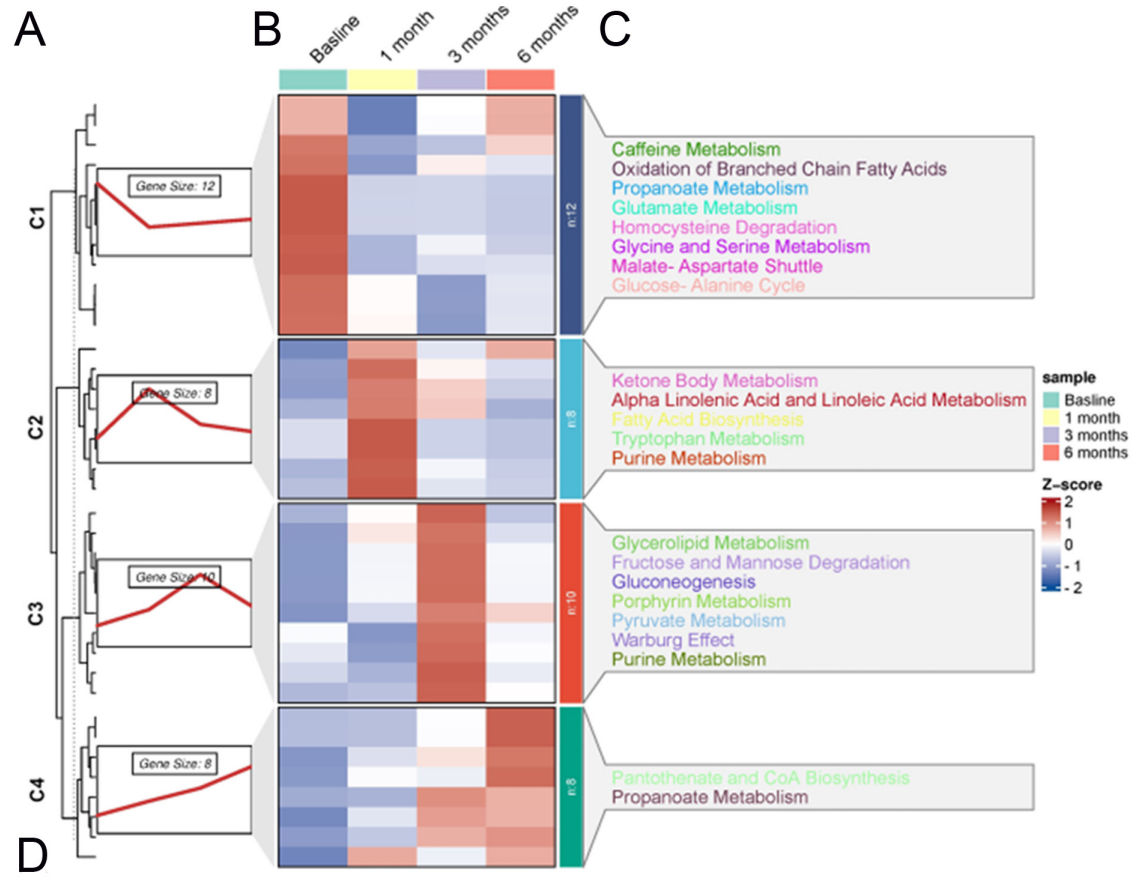

C1	Oxoglutarate	2-Ketobutyric acid	Succinic acid semialdehyde	2,4-Dihydroxypyrimidine-5-carboxylic acid	Arachidate
	Menaquinone	Propionylcarnitine (C3)	Paraxanthine	Uracil 5-carboxylate	Orotate
	Theophylline	1-Methylxanthine			
C2	N α -Acetyl-L-lysine	2-Hydroxycaproic acid	Acetylglycine	3-Hydroxybutanoate	
	Guanosine	N-Acetylglycine	Indoleacetic acid	Eicosapentaenoate	
C3	DL-Glyceraldehyde	Glyceraldehyde	Biliverdin	N-Formyl-L-methionine	Lactate
	4-Methylpyrazole	Indoxyl	Guanine	3-Indolepropionic acid	Benzoate
C4	Phthalic acid	Pantetheine	Oxamic acid	1-Methyl-2-pyrrolidone	
	Indoxyl sulfate	Dihydroxyfumarate	Hippurate	2-Piperidinone	

Figure 3

Time-series clustering, heat map, and pathway enrichment analysis. (A) Time-series clustering. Based on the core algorithm, fuzzy C-means custering, the metabolites with similar expression patterns were classified into four clusters. (B) Heat maps of metabolite concentration variations in the four clusters. (C) Metabolite enrichment analysis for each cluster based on the Small Molecule Pathway Database (SMPDB), and the top terms enriched with the lowest *P*-value are labeled. (D) The specific metabolite names of each cluster.

was negatively correlated with HOMA-IR. Pantetheine levels were significantly negatively correlated with BMI, HOMA-IR, and liver fat content. Oxamic acid levels were significantly negatively correlated with HOMA-IR and liver fat content. Dihydroxyfumarate was negatively correlated with liver fat content (Fig. 6). The correlations between the other 29 DEMs and clinical parameters during the entire postoperative follow-up period are shown in Supplementary Table 1 (see section on supplementary materials given at the end of this article).

Discussion

Through a non-targeted metabolomic approach, our longitudinal study of patients with obesity post-LSG revealed significant changes in metabolomic profiles at 1-, 3-, and 6-month postoperative time points. Some of the changed metabolites in this process were associated with different degrees of clinical metabolic improvement according to anthropometric and clinical parameters. Notably, we further analyzed the

Endocrine Connections (2024) **13** e240292
https://doi.org/10.1530/EC-24-0292

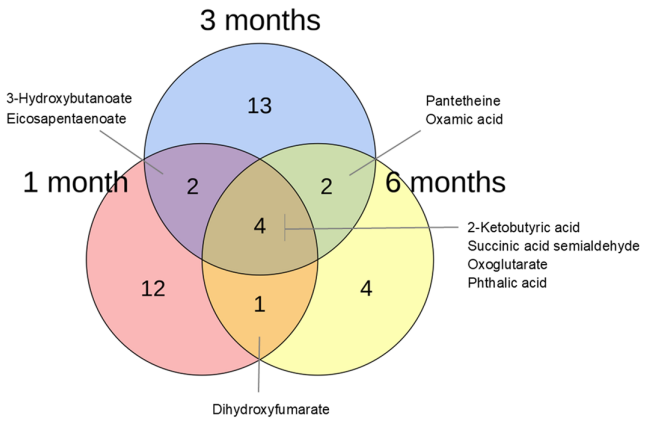

Figure 4

Venn plot of differentially expressed metabolites (DEMs) in three postoperative time periods.

metabolic pathways involved in these changes and found some potential biomarkers that were intimately related to clinical metabolic improvements.

Our results confirmed significant clinical metabolic improvement after LSG during the 6-month follow-up period, including weight loss, remission of insulin resistance, improvement of dyslipidemia, and a decrease in liver fat content. HOMA-IR, as an indicator of insulin resistance, showed a gradual downward trend at the three follow-up points after LSG, with significant differences compared with baseline. HbA1c, an indicator of blood glucose control, showed no significant decrease. This implies that the improvement in diabetes after LSG may begin with the remission of insulin resistance (IR). In addition, an increase in HDL-C levels was observed at the 6-month postoperative time point, but no statistically significant change was observed in TC, TG, and LDL-C levels, which means that the improvement of blood lipid profiles may require a longer process and may be greatly affected by postoperative dietary habits and lifestyle. Notably, liver fat content showed a gradually decreasing trend during the postoperative follow-up, suggesting that LSG can improve liver lipid metabolism; however, the underlying mechanisms remain unclear.

According to the principles of *P*-value <0.05, VIP values >1, and FC ≥ 2 or ≤ 0.5, we screened 38 DEMs that showed significant variations during follow-up compared to baseline. These metabolites were categorized into four clusters through time-series analysis, including upregulation types (continuous ascending, early ascending, and late ascending) and a downregulation type. Through metabolite enrichment analysis based on the SMPDB, in the upregulation type, we identified pantothenate and CoA biosynthesis, which are closely related to energy metabolism, fat synthesis and oxidation, and insulin resistance, as the most enriched pathway in the continuous ascending type (cluster 4). Pantothenate, also called vitamin B5, is a water-soluble vitamin required to sustain life. A recent study has shown that pantothenate protects against obesity via brown adipose tissue activation (17). Pantothenate derivatives have a good hypolipidemic effect in mice with hypothalamic obesity induced by aurothioglucose (18). Pantetheine, as the active form of pantothenate in the body, was found to be continuously elevated in our results, which was consistent with the metabolic improvement after LSG. Ketone body metabolism and alpha-linolenic acid and linoleic acid metabolism were the main metabolic pathways enriched in the early ascending type (cluster 2). Previous studies suggested that after bariatric surgery, a strong and early upregulation of catabolism and lipolytic activity occurred, and the end products of β-oxidation and ketogenesis increased, especially in the short-term period after surgery (19, 20, 21). Another study showed that the highest weight loss group had greater increases in serum ketone bodies after LSG than the lowest weight loss group (22). Our results were consistent with the above studies, which showed a rapid early rise of ketone body (3-hydroxybutanoate), followed by a slow decline after LSG, but consistently above the baseline. Eicosapentaenoate (EPA) is involved in alpha-linolenic acid and linoleic acid metabolism, which is an ω-3 polyunsaturated fatty acid that plays an important role in human health, such as in reducing the risk of cardiovascular disease, anti-inflammatory effects, and protection against lipemic-oxidative injury (23). In our study, although no significant correlation was found between EPA and clinical metabolic indicators, the early increase in EPA levels reflected the metabolic benefits of obesity after LSG. Moreover, the enrichment of glycerolipid metabolism, fructose and mannose degradation, and gluconeogenesis in the late ascending type (cluster 3) suggested that LSG altered carbohydrate and lipid metabolism. We observed an increase in glyceraldehyde (a key intermediate in glycolipid metabolism), but only in the first 3 months post-surgery. This can be explained by lipolysis, which has been reported to increase in the short term post surgery (24). Possible explanations for the gradual decline during further months after surgery can be a reduction in total lipids and their uptake by the liver, where they are used as a precursor of gluconeogenesis (25). In addition, fructose is converted to glucose in the liver (26). The plasma mannose levels were significantly up-regulated in obesity and potentially played a supplementary role in the development of IR (27). The degradation of fructose and mannose implied that the disorder of glucose metabolism in obesity was improved after LSG.

In the down-regulated metabolites, we identified caffeine metabolism, oxidation of branched-chain fatty acids, glutamate metabolism, and homocysteine degradation as the main enriched pathways (cluster 1). Two important applications of caffeine are metabolic phenotyping of cytochrome P450 1A2 (CYP1A2) and liver function testing (28). Caffeine metabolites, such as 1-methylxanthine and paraxanthine, can differentiate

Endocrine Connections (2024) **13** e240292
https://doi.org/10.1530/EC-24-0292

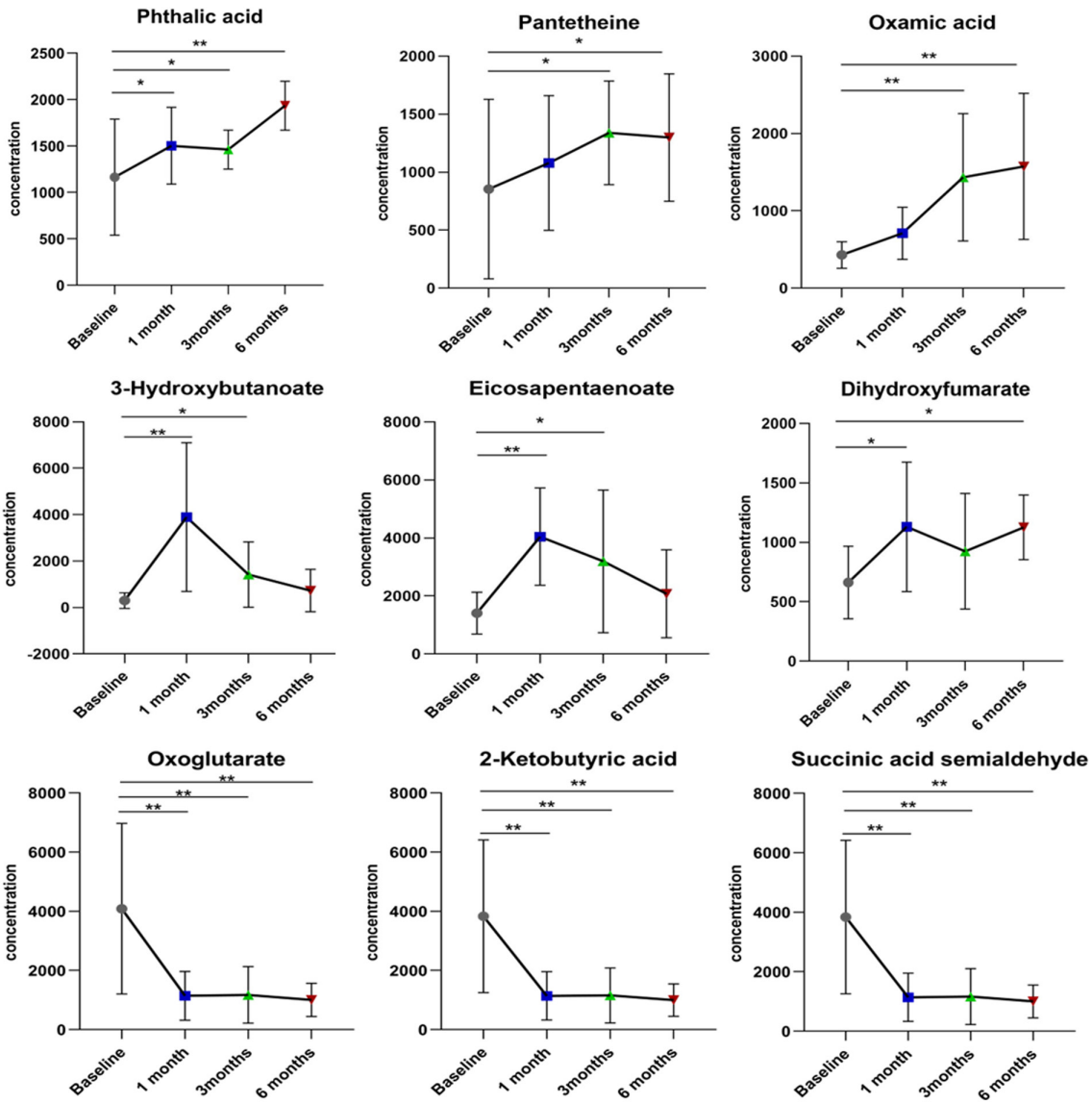

Figure 5

Variation trends of the nine continuously changing DEMs at all three postoperative time points.

the severity of early-stage liver disease (29). Total overnight salivary caffeine assessment in cirrhotic patients was significantly higher than in controls (30). The alteration in caffeine metabolism reflects the possible pathway of the effect of LSG on liver metabolism. Studies have shown that propionylcarnitine, an important molecule in branched-chain fatty acid oxidation, increases obesity and metabolic unwellness (31). In our study, propionylcarnitine (C3), an intermediate product of fatty acid metabolism, showed a decreasing trend after an improvement in obesity, which was consistent with previous reports. Moreover, to our knowledge, elevated plasma homocysteine is an independent risk factor for atherosclerosis (32). The enrichment of homocysteine degradation suggests that LSG may be significantly associated with an improvement in cardiovascular events.

From the DEM profiles and enriched pathways above, it was evident that the up-regulated metabolites post-LSG were mainly enriched in the pathways related to carbohydrate and lipid metabolism, while the down-regulated metabolites primarily correlated with amino acid metabolic pathways. Prior studies have reported that circulating amino acid levels are elevated in obesity and undergo a rapid decline following bariatric surgery due to reduced protein intake and amino acid absorption (33). Our results suggested that in the early postoperative period, the body's energy demand paradoxically increased due to stress responses and

Endocrine Connections (2024) **13** e240292
https://doi.org/10.1530/EC-24-0292

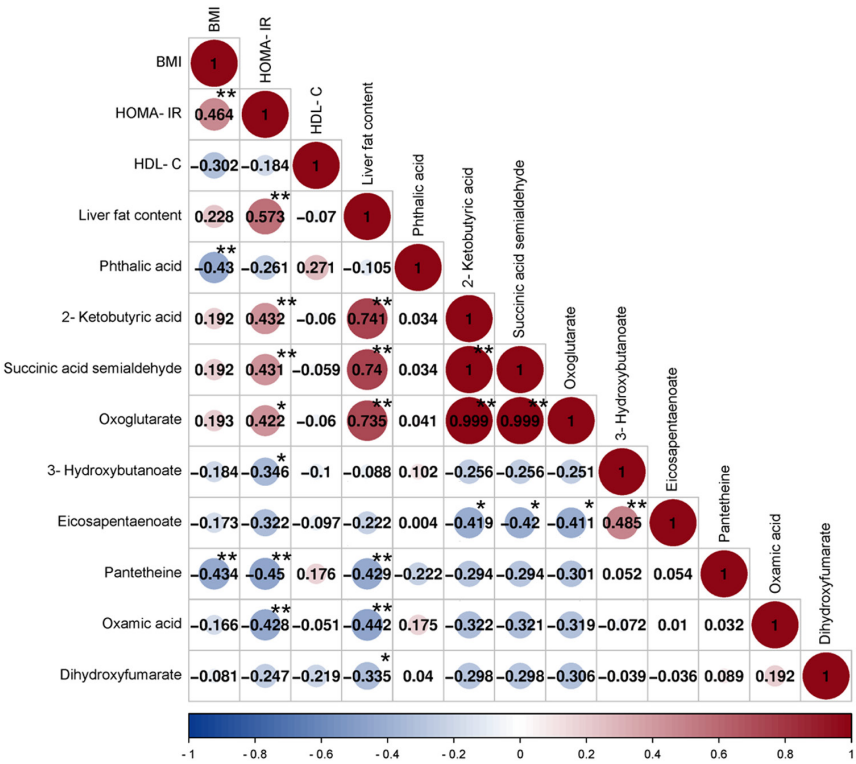

Figure 6

Correlation coefficient matrix diagram of the nine continuously changing DEMs and clinical metabolic parameters. *$P < 0.05$, **$P < 0.01$.

wound healing. To maintain energy homeostasis, the body significantly enhanced fat mobilization, thereby increasing lipolysis to provide energy. This process led to a massive accumulation of ketone bodies and β-oxidation metabolites. In the later stages of postoperative recovery, the lipolysis pathway tended to stabilize, leading to a decrease in ketone bodies and a relative increase in carbohydrate utilization, which promoted the production of glycolipid conversion intermediates (such as glyceraldehyde, as observed in our results). Overall, from the perspective of changes in metabolic pathways, the combined effects of diminished nutrient absorption and augmented mobilization of glucose and lipid metabolism may jointly contribute to the weight loss and metabolic benefits after LSG.

In all DEMs, compared with baseline, nine metabolites showed persistent differential expression at least at two postoperative time points. In addition to pantetheine, 3-hydroxybutanoate, and EPA have already mentioned above, oxoglutarate, 2-ketobutyric acid, succinic acid semialdehyde, phthalic acid, oxamic acid, and dihydroxyfumarate were included. Correlation analysis revealed that some of these metabolites were significantly correlated with BMI, HOMA-IR, and liver fat content. Therefore, we analyzed the possible roles and potential pathways of these metabolites in obesity, glycometabolism, and lipid metabolism.

Oxoglutarate, also known as α-ketoglutarate (α-KG), is an important metabolic intermediate that plays a key role in the tricarboxylic acid (TCA) cycle. Diabetes can cause significant increases in the levels of α-KG (34). The study of the circulating metabolome reveals α-KG as a predictor of morbid obesity associated with NAFLD, and plasma α-KG levels are significantly decreased in lean controls compared with obese patients (35). A nuclear magnetic resonance study also indicated increased hepatic TCA cycle flux in human NAFLD (36). A study in the livers of high-fat diet mice demonstrated that increased TCA cycle flux was associated with hepatic steatosis (37). In addition, the concentrations of glutamine, α-KG, citrate, and pyruvate were higher in patients with non-alcoholic steatohepatitis (NASH) than in patients without NASH, which may be related to the impairment of the TCA cycle. Activation of glutaminolysis may be the source of increased α-KG levels in patients with NASH (38, 39). These metabolic responses may be remodeled following the resolution of liver damage through massive weight loss (40). Our study found that α-KG decreased after LSG, which showed a positive correlation with liver fat content and HOMA-IR. One reason may be the reduced absorption of nutrients by the gastrointestinal tract after LSG, and another important reason may be related to the improvement of metabolic state after LSG, leading to the return of TCA circulation from high flux to normal with a reduction of α-KG. As recent studies reported, α-KG can be used as a signal molecule to control hepatic gluconeogenesis via the AKG-serpina1e pathway, which decreased blood glucose in mice (41). It can also stimulate muscle hypertrophy and fat loss through oxoglutarate receptor 1 (OXGR1)-dependent adrenal activation (42). These findings suggest that

Endocrine Connections (2024) **13** e240292
https://doi.org/10.1530/EC-24-0292

α-KG holds promising potential as a novel biomarker and therapeutic target for combating obesity and its associated comorbidities.

2-Ketobutyric acid, also known as 2-ketobutyrate or 2-oxobutyrate, is involved in the metabolism of various amino acids. It is an intermediate in the TCA cycle and is involved in the process of glucose oxidation for energy. Studies have shown that 2-ketobutyric acid can affect the level of mitochondrial substrate-level phosphorylation (43). Although only a few studies have reported the anti-obesity effect of 2-ketobutyrate, a longitudinal cohort in children aged 5–16 years showed that reduced concentrations of 2-ketobutyrate were associated with insulin resistance (44). In addition, α-hydroxybutyrate, converted from 2-ketobutyrate in adipocytes, modulates lipid metabolism both *in vitro* and *in vivo* (45). In high-fat diet-fed mice, the metabolomic analysis of lactis IDCC 4301 intracellular metabolite profiles suggested that 2-ketobutyrate could be a potential target compound against obesity, mediating the bacterial anti-obesity effects (46).

At present, there are limited studies on succinic acid semialdehyde (SSA), mainly focusing on its synthetic metabolites succinic acid (SA) and gamma-aminobutyric acid (GABA). SSA is an extremely efficient substrate that energizes mitochondria during normoxia (47). SA is produced from SSA by the catalysis of succinic semialdehyde dehydrogenase, which can participate in the TCA cycle and combine with the electron transport chain to produce a large amount of free energy (47, 48). A previous genome-wide association study (GWAS) on obese/overweight women reported that SA was positively associated with obesity (49). Our results showed a decline in SSA when obesity improved after SG surgery, which supports this claim. In addition, GABA is produced from SSA through a series of enzymatic reactions (50). Treatment with GABA mitigated high-fat diet-induced hyperglycemia by repairing muscular oxidative stress and plasma free amino acid disorders in mice (51). In high glucose concentrations, SSA acts as a cell-permeant 'GABA-shunt' metabolite that promotes islet GABA metabolism, increases ATP and the ATP/ADP ratio, depolarizes β-cells, and stimulates insulin secretion (52). However, whether there is a causal relationship between SSA and insulin resistance improvement remains uncertain.

Oxamic acid is a pyruvate analog that can competitively inhibit lactate dehydrogenase (LDH)-catalyzed conversion of pyruvate into lactate. Oxamate (OXA), its salt form, acts as an LDH inhibitor and can limit cancer cell migration induced by inflammatory processes (53). As a key enzyme in glycolysis, LDH plays an important role in the regulation of glycometabolism. In db/db mice, OXA can improve glycemic control and insulin sensitivity via inhibition of tissue lactate production (54). In our study, OXA showed a continuous increasing trend after LSG, but its direct contribution to metabolic improvements, such as the reduction of liver fat content, requires further investigation.

Phthalic acid (PA) is a synthetic organic compound, which is mainly obtained from the external environment. As external precursors of PA, phthalates are known endocrine disruptors and oxidant stressors, and exposure has been associated with obesity and insulin resistance (55). Their accumulation in adipose tissue is due to their lipophilic nature, which further increases the retention of other lipophilic chemicals (56). A 10-year prospective cohort study showed that certain phthalate metabolites in urine were associated with modestly greater weight gain in a dose–response manner (57). However, in our study, the concentration of PA in serum did not decrease but increased after LSG, which was not consistent with the weight loss and metabolic improvement status. Possible reasons are as follows. First, phthalates are widely used in medical devices, capsule drugs, food packaging, cosmetics, textiles, etc. (58). Patients after bariatric surgery often need to take acid-suppressing and stomach-protecting drugs. The increased levels of PA in the bloodstream of these postoperative patients may be related to the drug capsules or other external exposures to phthalates, rather than the result of surgery. In addition, rapid weight loss is always accompanied by the cleavage of a large number of fat cells owing to the lipophilic nature of PA, resulting in the release of accumulated PA into the blood. We only detected PA in the bloodstream, and further tests of the liver and urine are necessary.

As previous studies mainly focused on European and American populations, our study elucidated the metabolome characteristics in Chinese obese populations after LSG. The longitudinal follow-up at three time points enhanced the reliability of the results. However, in human samples, food or drug intake and other environmental exposures may affect serum metabolite concentrations. Considering the limitation of sample size, it is difficult to conduct subgroup analysis. Although untargeted metabolomics offers significant advantages in revealing novel metabolic signatures and discovering potential biomarkers, its quantitative accuracy is relatively limited compared to targeted metabolomics approaches. The targeted metabolomics validation in a larger sample population is needed in the future. Moreover, the role of these metabolites in metabolic improvement and their specific mechanisms require more in-depth in vivo and in vitro experiments to prove.

Conclusions

In summary, this study identified significant changes in the serum metabolomic profile at 1-, 3-, and 6-month post surgery compared to pre-surgery, which

opened up new insights into the biomarkers and mechanisms of metabolic improvement in obesity and related diseases after LSG.

Supplementary materials

This is linked to the online version of the paper at https://doi.org/10.1530/EC-24-0292.

Declaration of interest

The authors declare that there is no conflict of interest that could be perceived as prejudicing the impartiality of the research reported.

Funding

This research was supported by the National Science and Technology Major Project (Grant No. 2023ZD0508703 to HB); National Natural Science Foundation of China (Grant no. 82370870 to HB); Science and Technology Commission of Shanghai Municipality (Grant no. 22Y31900302 to HB); Shanghai Municipal Health Commission (Grant no. 202240295 to HB); and the Youth Fund of the National Natural Science Foundation of China (Grant no. 82100827 to YH).

Acknowledgements

We thank Lei Zhang, School of Life Sciences, Core Facility of Biomedical Sciences, Xiamen University, for the kind support with LC-MS experiments.

References

1 Kheniser K, Saxon DR & Kashyap SR. Long-term weight loss strategies for obesity. *Journal of Clinical Endocrinology and Metabolism* 2021 **106** 1854–1866. (https://doi.org/10.1210/clinem/dgab091)

2 Blüher M, Aras M, Aronne LJ, Batterham RL, Giorgino F, Ji L, Pietiläinen KH, Schnell O, Tonchevska E & Wilding JPH. New insights into the treatment of obesity. *Diabetes, Obesity and Metabolism* 2023 **25** 2058–2072. (https://doi.org/10.1111/dom.15077)

3 Elmaleh-Sachs A, Schwartz JL, Bramante CT, Nicklas JM, Gudzune KA & Jay M. Obesity management in adults: a review. *JAMA* 2023 **330** 2000–2015. (https://doi.org/10.1001/jama.2023.19897)

4 Çeler Ö, Er HC, Sancak S, Çırak E, Özdemir A, Sertbaş Y, Karip AB, Esen Bulut N, Aydın MT, Altun H, *et al.* The effects of laparoscopic sleeve gastrectomy (LSG) on obesity-related type 2 diabetes mellitus: a prospective observational study from a single center. *Obesity Surgery* 2023 **33** 2695–2701. (https://doi.org/10.1007/s11695-023-06707-y)

5 Vigilante A, Signorini F, Marani M, Paganini V, Viscido G, Navarro L, Obeide L & Moser F. Impact on dyslipidemia after laparoscopic sleeve gastrectomy. *Obesity Surgery* 2018 **28** 3111–3115. (https://doi.org/10.1007/s11695-018-3343-4)

6 Blanco DG, Funes DR, Giambartolomei G, Lo Menzo E, Szomstein S & Rosenthal RJ. Laparoscopic sleeve gastrectomy versus Roux-en-Y gastric bypass in cardiovascular risk reduction: a match control study. *Surgery for Obesity and Related Diseases* 2019 **15** 14–20. (https://doi.org/10.1016/j.soard.2018.09.488)

7 Głuszyńska P, Lemancewicz D, Dzięcioł JB & Razak Hady H. Non-alcoholic fatty liver disease (NAFLD) and bariatric/metabolic surgery as its treatment option: a review. *Journal of Clinical Medicine* 2021 **10** 5721. (https://doi.org/10.3390/jcm10245721)

8 Naik RD, Choksi YA & Vaezi MF. Consequences of bariatric surgery on oesophageal function in health and disease. *Nature Reviews. Gastroenterology and Hepatology* 2016 **13** 111–119. (https://doi.org/10.1038/nrgastro.2015.202)

9 Perdomo CM, Cohen RV, Sumithran P, Clément K & Frühbeck G. Contemporary medical, device, and surgical therapies for obesity in adults. *Lancet* 2023 **401** 1116–1130. (https://doi.org/10.1016/S0140-6736(22)02403-5)

10 Buchwald H. The evolution of metabolic/bariatric surgery. *Obesity Surgery* 2014 **24** 1126–1135. (https://doi.org/10.1007/s11695-014-1354-3)

11 Liu R, Hong J, Xu X, Feng Q, Zhang D, Gu Y, Shi J, Zhao S, Liu W, Wang X, *et al.* Gut microbiome and serum metabolome alterations in obesity and after weight-loss intervention. *Nature Medicine* 2017 **23** 859–868. (https://doi.org/10.1038/nm.4358)

12 Flynn CR, Albaugh VL, Cai S, Cheung-Flynn J, Williams PE, Brucker RM, Bordenstein SR, Guo Y, Wasserman DH & Abumrad NN. Bile diversion to the distal small intestine has comparable metabolic benefits to bariatric surgery. *Nature Communications* 2015 **6** 7715. (https://doi.org/10.1038/ncomms8715)

13 Qiu S, Cai Y, Yao H, Lin C, Xie Y, Tang S & Zhang A. Small molecule metabolites: discovery of biomarkers and therapeutic targets. *Signal Transduction and Targeted Therapy* 2023 **8** 132. (https://doi.org/10.1038/s41392-023-01399-3)

14 Pantelis AG. Metabolomics in bariatric and metabolic surgery research and the potential of deep learning in bridging the gap. *Metabolites* 2022 **12** 458. (https://doi.org/10.3390/metabo12050458)

15 Ha J, Jang M, Kwon Y, Park YS, Park DJ, Lee J-H, Lee H-J, Ha TK, Kim Y-J, Han S-M, *et al.* Metabolomic profiles predict diabetes remission after bariatric surgery. *Journal of Clinical Medicine* 2020 **9** 3897. (https://doi.org/10.3390/jcm9123897)

16 Zhang Y, Shi C, Wu H, Yan H, Xia M, Jiao H, Zhou D, Wu W, Zhong M, Lou W, *et al.* Characteristics of changes in plasma proteome profiling after sleeve gastrectomy. *Frontiers in Endocrinology* 2024 **15** 1330139. (https://doi.org/10.3389/fendo.2024.1330139)

17 Zhou H, Zhang H, Ye R, Yan C, Lin J, Huang Y, Jiang X, Yuan S, Chen L, Jiang R, *et al.* Pantothenate protects against obesity via brown adipose tissue activation. *American Journal of Physiology. Endocrinology and Metabolism* 2022 **323** E69–E79. (https://doi.org/10.1152/ajpendo.00293.2021)

18 Naruta E & Buko V. Hypolipidemic effect of pantothenic acid derivatives in mice with hypothalamic obesity induced by aurothioglucose. *Experimental and Toxicologic Pathology* 2001 **53** 393–398. (https://doi.org/10.1078/0940-2993-00205)

19 Friedrich N, Budde K, Wolf T, Jungnickel A, Grotevendt A, Dreßler M, Völzke H, Blüher M, Nauck M, Lohmann T, *et al.* Short-term changes of the urine metabolome after bariatric surgery. *OMICS* 2012 **16** 612–620. (https://doi.org/10.1089/omi.2012.0066)

20 Mendonça Machado N, Torrinhas RS, Sala P, Ishida RK, Guarda IFMS, Moura EGH, Sakai P, Santo MA & Linetzky Waitzberg D. Type 2 diabetes metabolic improvement after Roux-en-Y gastric bypass may include a compensatory mechanism that balances fatty acid β and ω oxidation. *JPEN* 2020 **44** 1417–1427. (https://doi.org/10.1002/jpen.1960)

21 Samczuk P, Luba M, Godzien J, Mastrangelo A, Hady HR, Dadan J, Barbas C, Gorska M, Kretowski A & Ciborowski M. "Gear mechanism" of bariatric interventions revealed by untargeted metabolomics. *Journal of Pharmaceutical and Biomedical Analysis* 2018 **151** 219–226. (https://doi.org/10.1016/j.jpba.2018.01.016)

22 Miller WM, Ziegler KM, Yilmaz A, Saiyed N, Ustun I, Akyol S, Idler J, Sims MD, Maddens ME & Graham SF. Association of metabolomic biomarkers with sleeve gastrectomy weight loss outcomes. *Metabolites* 2023 **13** 506. (https://doi.org/10.3390/metabo13040506)

23 Kumar SA, Sudhahar V & Varalakshmi P. Attenuation of serum lipid abnormalities and cardiac oxidative stress by eicosapentaenoate–lipoate (EPA–LA) derivative in experimental hypercholesterolemia. *Clinica Chimica Acta* 2005 **355** 197–204. (https://doi.org/10.1016/j.cccn.2005.01.003)

24 Hansen M, Lund MT, Gregers E, Kraunsøe R, Van Hall G, Helge JW & Dela F. Adipose tissue mitochondrial respiration and lipolysis before and after a weight loss by diet and RYGB. *Obesity* 2015 **23** 2022–2029. (https://doi.org/10.1002/oby.21223)

25 Rui L. Energy metabolism in the liver. *Comprehensive Physiology* 2014 **4** 177–197. (https://doi.org/10.1002/cphy.c130024)

26 Dashty M. A quick look at biochemistry: carbohydrate metabolism. *Clinical Biochemistry* 2013 **46** 1339–1352. (https://doi.org/10.1016/j.clinbiochem.2013.04.027)

27 Lee S, Zhang C, Kilicarslan M, Piening BD, Bjornson E, Hallström BM, Groen AK, Ferrannini E, Laakso M, Snyder M, *et al.* Integrated network analysis reveals an association between plasma mannose levels and insulin resistance. *Cell Metabolism* 2016 **24** 172–184. (https://doi.org/10.1016/j.cmet.2016.05.026)

28 Grzegorzewski J, Bartsch aF, Köller A & König M. Pharmacokinetics of caffeine: a systematic analysis of reported data for application in metabolic phenotyping and liver function testing. *Frontiers in Pharmacology* 2021 **12** 752826. (https://doi.org/10.3389/fphar.2021.752826)

29 Xu R, He L, Vatsalya V, Ma X, Kim S, Mueller EG, Feng W, McClain CJ & Zhang X. Metabolomics analysis of urine from patients with alcohol-associated liver disease reveals dysregulated caffeine metabolism. *American Journal of Physiology. Gastrointestinal and Liver Physiology* 2023 **324** G142–G154. (https://doi.org/10.1152/ajpgi.00228.2022)

30 Tarantino G, Conca P, Capone D, Gentile A, Polichetti G & Basile V. Reliability of total overnight salivary caffeine assessment (TOSCA) for liver function evaluation in compensated cirrhotic patients. *European Journal of Clinical Pharmacology* 2006 **62** 605–612. (https://doi.org/10.1007/s00228-006-0146-7)

31 Libert DM, Nowacki AS & Natowicz MR. Metabolomic analysis of obesity, metabolic syndrome, and type 2 diabetes: amino acid and acylcarnitine levels change along a spectrum of metabolic wellness. *PeerJ* 2018 **6** e5410. (https://doi.org/10.7717/peerj.5410)

32 Almer G, Opriessnig P, Wolinski H, Sommer G, Diwoky C, Lechleitner M, Kolb D, Bubalo V, Brunner MS, Schwarz AN, *et al.* Deficiency of B vitamins leads to cholesterol-independent atherogenic transformation of the aorta. *Biomedicine and Pharmacotherapy* 2022 **154** 113640. (https://doi.org/10.1016/j.biopha.2022.113640)

33 Vaz M, Pereira SS & Monteiro MP. Metabolomic signatures after bariatric surgery – a systematic review. *Reviews in Endocrine and Metabolic Disorders* 2022 **23** 503–519. (https://doi.org/10.1007/s11154-021-09695-5)

34 Nie Q, Chen H, Hu J, Gao H, Fan L, Long Z & Nie S. Arabinoxylan attenuates type 2 diabetes by improvement of carbohydrate, lipid, and amino acid metabolism. *Molecular Nutrition and Food Research* 2018 **62** e1800222. (https://doi.org/10.1002/mnfr.201800222)

35 Rodríguez-Gallego E, Guirro M, Riera-Borrull M, Hernández-Aguilera A, Mariné-Casadó R, Fernández-Arroyo S, Beltrán-Debón R, Sabench F, Hernández M, del Castillo D, *et al.* Mapping of the circulating metabolome reveals α-ketoglutarate as a predictor of morbid obesity-associated non-alcoholic fatty liver disease. *International Journal of Obesity* 2015 **39** 279–287. (https://doi.org/10.1038/ijo.2014.53)

36 Sunny NE, Parks EJ, Browning JD & Burgess SC. Excessive hepatic mitochondrial TCA cycle and gluconeogenesis in humans with nonalcoholic fatty liver disease. *Cell Metabolism* 2011 **14** 804–810. (https://doi.org/10.1016/j.cmet.2011.11.004)

37 Patterson RE, Kalavalapalli S, Williams CM, Nautiyal M, Mathew JT, Martinez J, Reinhard MK, McDougall DJ, Rocca JR, Yost RA, *et al.* Lipotoxicity in steatohepatitis occurs despite an increase in tricarboxylic acid cycle activity. *American Journal of Physiology. Endocrinology and Metabolism* 2016 **310** E484–E494. (https://doi.org/10.1152/ajpendo.00492.2015)

38 Cabré N, Luciano-Mateo F, Chapski DJ, Baiges-Gaya G, Fernández-Arroyo S, Hernández-Aguilera A, Castañé H, Rodríguez-Tomàs E, París M, Sabench F, *et al.* Laparoscopic sleeve gastrectomy in patients with severe obesity restores adaptive responses leading to nonalcoholic steatohepatitis. *International Journal of Molecular Sciences* 2022 **23** 7830. (https://doi.org/10.3390/ijms23147830)

39 Cabré N, Luciano-Mateo F, Chapski DJ, Baiges-Gaya G, Fernández-Arroyo S, Hernández-Aguilera A, Castañé H, Rodríguez-Tomàs E, París M, Sabench F, *et al.* WITHDRAWN: glutaminolysis-induced mTORC1 activation drives non-alcoholic steatohepatitis progression. *Journal of Hepatology* 2021. (https://doi.org/10.1016/j.jhep.2021.04.037)

40 Cabré N, Luciano-Mateo F, Baiges-Gayà G, Fernández-Arroyo S, Rodríguez-Tomàs E, Hernández-Aguilera A, París M, Sabench F, Del Castillo D, López-Miranda J, *et al.* Plasma metabolic alterations in patients with severe obesity and non-alcoholic steatohepatitis. *Alimentary Pharmacology and Therapeutics* 2020 **51** 374–387. (https://doi.org/10.1111/apt.15606)

41 Yuan Y, Zhu C, Wang Y, Sun J, Feng J, Ma Z, Li P, Peng W, Yin C, Xu G, *et al.* α-Ketoglutaric acid ameliorates hyperglycemia in diabetes by inhibiting hepatic gluconeogenesis via serpina1e signaling. *Science Advances* 2022 **8** eabn2879. (https://doi.org/10.1126/sciadv.abn2879)

42 Yuan Y, Xu P, Jiang Q, Cai X, Wang T, Peng W, Sun J, Zhu C, Zhang C, Yue D, *et al.* Exercise-induced α-ketoglutaric acid stimulates muscle hypertrophy and fat loss through OXGR1-dependent adrenal activation. *EMBO Journal* 2020 **39** e108434. (https://doi.org/10.15252/embj.2019103304)

43 Bui D, Ravasz D & Chinopoulos C. The effect of 2-ketobutyrate on mitochondrial substrate-level phosphorylation. *Neurochemical Research* 2019 **44** 2301–2306. (https://doi.org/10.1007/s11064-019-02759-8)

44 Hosking J, Pinkney J, Jeffery A, Cominetti O, Da Silva L, Collino S, Kussmann M, Hager J & Martin FP. Insulin resistance during normal child growth and development is associated with a distinct blood metabolic phenotype (Earlybird 72). *Pediatric Diabetes* 2019 **20** 832–841. (https://doi.org/10.1111/pedi.12884)

45 Adams SH. Emerging perspectives on essential amino acid metabolism in obesity and the insulin-resistant state. *Advances in Nutrition* 2011 **2** 445–456. (https://doi.org/10.3945/an.111.000737)

46 Ban OH, Lee M, Bang WY, Nam EH, Jeon HJ, Shin M, Yang J & Jung YH. Bifidobacterium lactis IDCC 4301 exerts anti-obesity effects in high-fat diet-fed mice model by regulating lipid metabolism. *Molecular Nutrition and Food Research* 2023 **67** e2200385. (https://doi.org/10.1002/mnfr.202200385)

47 Ravasz D, Kacso G, Fodor V, Horvath K, Adam-Vizi V & Chinopoulos C. Catabolism of GABA, succinic semialdehyde or gamma-hydroxybutyrate through the GABA shunt impair mitochondrial substrate-level phosphorylation. *Neurochemistry International* 2017 **109** 41–53. (https://doi.org/10.1016/j.neuint.2017.03.008)

48 Ives SJ, Zaleski KS, Slocum C, Escudero D, Sheridan C, Legesse S, Vidal K, Lagalwar S & Reynolds TH. The effect of succinic acid on the metabolic profile in high-fat diet-induced obesity and insulin resistance. *Physiological Reports* 2020 **8** e14630. (https://doi.org/10.14814/phy2.14630)

49 Kim MJ, Kim JH, Kim MS, Yang HJ, Lee M & Kwon DY. Metabolomics associated with genome-wide association study related to the basal metabolic rate in overweight/obese Korean women. *Journal of Medicinal Food* 2019 **22** 499–507. (https://doi.org/10.1089/jmf.2018.4310)

50 Tamarit-Rodriguez J. Metabolic role of GABA in the secretory function of pancreatic β-cells: its hypothetical implication in β-cell degradation in type 2 diabetes. *Metabolites* 2023 **13** 697. (https://doi.org/10.3390/metabo13060697)

51 Xie ZX, Xia SF, Qiao Y, Shi YH & Le GW. Effect of GABA on oxidative stress in the skeletal muscles and plasma free amino acids in mice fed high-fat diet. *Journal of Animal Physiology and Animal Nutrition* 2015 **99** 492–500. (https://doi.org/10.1111/jpn.12254)

52 Pizarro-Delgado J, Braun M, Hernández-Fisac I, Martín-Del-Río R & Tamarit-Rodriguez J. Glucose promotion of GABA metabolism contributes to the stimulation of insulin secretion in β-cells. *Biochemical Journal* 2010 **431** 381–389. (https://doi.org/10.1042/BJ20100714)

53 Forkasiewicz A, Stach W, Wierzbicki J, Stach K, Tabola R, Hryniewicz-Jankowska A & Augoff K. Effect of LDHA inhibition on TNF-α-induced cell migration in esophageal cancers. *International Journal of Molecular Sciences* 2022 **23** 16062. (https://doi.org/10.3390/ijms232416062)

54 Ye W, Zheng Y, Zhang S, Yan L, Cheng H & Wu M. Oxamate improves glycemic control and insulin sensitivity via inhibition of tissue lactate production in db/db mice. *PLoS One* 2016 **11** e0150303. (https://doi.org/10.1371/journal.pone.0150303)

55 Stahlhut RW, van Wijngaarden E, Dye TD, Cook S & Swan SH. Concentrations of urinary phthalate metabolites are associated with increased waist circumference and insulin resistance in adult U.S. males. *Environmental Health Perspectives* 2007 **115** 876–882. (https://doi.org/10.1289/ehp.9882)

56 Vandenberg LN, Colborn T, Hayes TB, Heindel JJ, Jacobs DR, Lee D-H, Shioda T, Soto AM, vom Saal FS, Welshons WV, *et al.* Hormones and endocrine-disrupting chemicals: low-dose effects and nonmonotonic dose responses. *Endocrine Reviews* 2012 **33** 378–455. (https://doi.org/10.1210/er.2011-1050)

57 Song Y, Hauser R, Hu FB, Franke AA, Liu S & Sun Q. Urinary concentrations of bisphenol A and phthalate metabolites and weight change: a prospective investigation in US women. *International Journal of Obesity* 2014 **38** 1532–1537. (https://doi.org/10.1038/ijo.2014.63)

58 Šimunović A, Tomić S & Kranjčec K. Medical devices as a source of phthalate exposure: a review of current knowledge and alternative solutions. *Arhiv za Higijenu Rada i Toksikologiju* 2022 **73** 179–190. (https://doi.org/10.2478/aiht-2022-73-3639)